



<http://greatlakescenter.buffalostate.edu/>

Lake Ontario *Cladophora* dynamics: from microscale nutrient concentrations to satellite imagery

Technical Report

Principal Investigator: Christopher Pennuto

Great Lakes Center

SUNY Buffalo State

1300 Elmwood Ave, Buffalo, New York USA 14222

March 2020

Suggested citation for the report:

Pennuto, CM. 2020. Lake Ontario *Cladophora* dynamics: from microscale nutrient concentrations to satellite imagery. Technical Report. Great Lakes Center, SUNY Buffalo State, Buffalo, NY. Available at:

Summary

Cladophora remains a nuisance algae across the Great Lakes region, and predicting how much and where it occurs is critical to understand its potential impacts to lake health and local economies. We investigated *Cladophora* growth dynamics with fine-scale spatiotemporal resolution, and coupled those findings with satellite data to improve predictive power of a *Cladophora* growth model (CGM). We found the nearshore zone in western Lake Ontario was a very dynamic zone, with multiple upwelling events, while at the same time the zone of *Cladophora* growth (out to 9 m depth) was well-mixed and chemically homogeneous. There were large changes in nutrient levels throughout the growing season, but those changes were consistent across all depths. In this particular year and location, *Cladophora* biomass was not particularly high, even though light, substrate, and nutrient conditions would suggest it should have been. Internal tissue carbon and nitrogen content declined over the growing season, as did chlorophyll *a* content, but phosphorus levels in tissues remained unchanged. We did not detect an appreciable mussel or *Cladophora* effect on microscale nutrient concentrations over the 90-day sampling period. Maximum biomass was found at the 3 m transect, but was most consistent at the 6 m contour. Biomass of *Cladophora* rarely reached nuisance levels (e.g., 50 g/m²) and we did not witness an obvious sloughing event. Data-sharing with researchers at Michigan Technological Research Institute resulted in improvements to the Great Lakes *Cladophora* Growth Model (GLCGM).

Background

The resurgence of nuisance levels of the benthic alga, *Cladophora glomerata*, is occurring across the Great Lakes, exclusive of Lake Superior. Although *Cladophora* overgrowth led to use impairment for Great Lakes beaches as early as the 1930's, pollution abatement technologies in the 1970/1980's succeeded in reducing algal biomass to below nuisance levels via reductions in phosphorus concentrations (e.g., Auer 2014). In Lake Ontario, open water, soluble reactive phosphorus (SRP) concentration dropped dramatically beginning in 1972 from an average of about 13 µg P/L to the current and fairly stable mean near 2 µg P/L (Dove and Chapra 2015). Although *Cladophora* levels declined with declining SRP levels, these low, lakewide SRP level have not curtailed *Cladophora* growth in recent years (Pennuto et al. 2012a, Dayton et al. 2014, Bootsma et al. 2015, Howell and Dove 2017, Watkins et al. 2017). Several works suggest that ecosystem changes coincident with the colonization of the Great Lakes by dreissenid mussels plays a role in the current *Cladophora* resurgence (e.g., Ozersky et al. 2009, Kuczynski et al. 2016).

Ecosystem engineering activities of dreissenid mussels lead to three habitat changes favorable for *Cladophora* growth; during feeding, mussels filter out small particulate matter, leading to increased light penetration at depth, their shells and byssal thread attachments provide firm and stable substrates

for algal attachment, and mussel food processing releases bioavailable P for uptake by benthic algae (Dayton et al. 2014, Kuczynski et al. 2016). Understanding these three habitat contexts (i.e., light levels, substrate availability, and bioavailable nutrient concentrations) formed the basis for the 2018 CSMI activities for Lake Ontario, and for which an EPA dive team and USGS laboratory personnel partnered. The main activities currently underway in Lake Ontario seek to provide data on these three variables for informing and validating a lake wide water quality model and the Great Lakes *Cladophora* growth model (CGM) by collecting field data from three nearshore locations on a monthly basis. Although a large suite of environmental data is being collected, greater temporal resolution of *Cladophora* growth dynamics will inform both the CGM as well as efforts to predict algal coverage and biomass via remote sensing (R. Shuchman, personal comm.).

This current work performed high resolution spatiotemporal sampling of water column nutrients, algal tissue nutrients, dreissenid mussel population conditions, and water column profiles. Our main objectives were to:

- 1) document *Cladophora* % coverage, mat height, biomass, and nutrient content at 3 depths (3, 6, and 9 m) on 10 dates over the growing season within the sampling area near Olcott, NY where high algal abundance is documented (Fig. 1),
- 2) document *Dreissena* % cover, density, and biomass (g/m^2) at 3 depths (3, 6, and 9 m) on 10 dates within the sampling area near Olcott, NY,
- 3) document nearbed and nearsurface concentrations of SRP at the same 10 locations for the above *Cladophora* and dreissenid collections, and
- 4) coordinate collections with researchers at Michigan Technical Research Institute to validate satellite representation of coverage and biomass changes with high temporal resolution. See technical report in Appendix A (MTRI 2020).

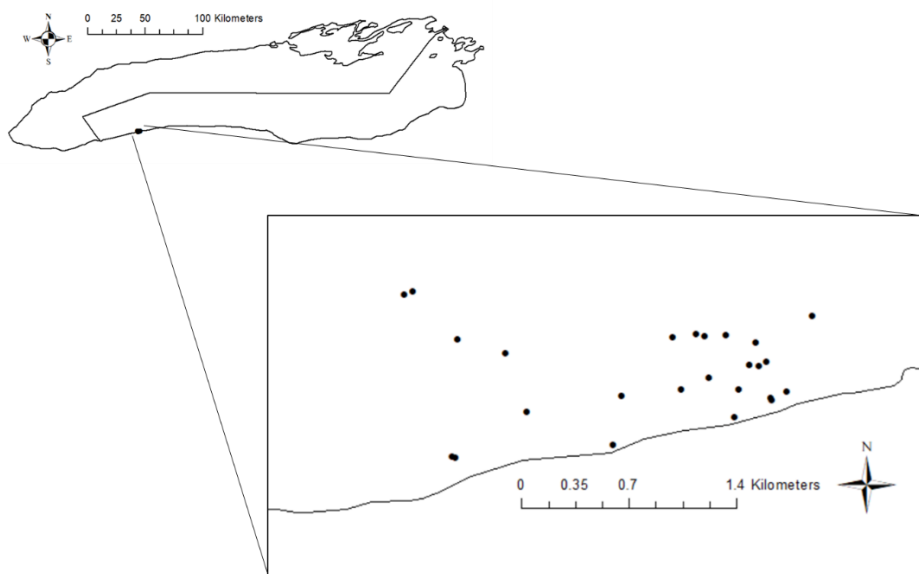


Figure 1. Locations for sample collections at 3, 6, and 9 m depth contours. Every 10 days, divers collected benthic water and benthos air-lift samples and a boat crew collections surface water and profile data.

Methods

Replicate ($n = 5$) *Cladophora* and dreissenid mussel samples were retrieved by divers using an air-lift sampler every 10 days from 3 depth contours in nearshore Lake Ontario. Additionally, a boat crew collected surface water samples and an array of profile data from each dive site.

Profiles

At each dive site on each date, a surface crew collected a single water sample using a field-rinsed van Dorn bottle from 1 m depth. The water was field-filtered (GF/C) into a 125 mL poly bottle and stored on ice in a cooler until returning to the lab. Once in the lab, water samples were frozen until shipment to the National Water Quality Lab at Heidelberg University (NCWQR) for processing. Secchi disc depth was determined. Temperature, conductivity, and oxygen profiles were collected using a YSI Quanta meter, with D.O. calibrated according to manufacturer's instructions prior to each field day. Bottom temperature was also obtained from 3 anchored temperature loggers (Optic Tidbit®), one each at 3, 6, and 9 m. Light penetration was obtained using a Li-Cor Model LI-193 with spherical quantum sensor.

Nearbed water chemistry

Once on the bottom, divers determined the predominant water flow direction by watching a stream of bubbles ascend toward the surface. The main current direction was then used to dictate on which side of a *Cladophora/Dreissena*-encrusted cobble water samples would be collected. The objective was to collect water within 2-5 cm of the substrate surface, or from within a *Cladophora* patch, at a location 'upcurrent' from, directly over, and 'downcurrent' from the selected cobble. Divers searched for isolated cobbles surrounded by some bare substrate (e.g., uncolonized bedrock, sand patch, or blanket of mussel shell fragments) before making collections. Triplicate water samples were sucked into 200-mL syringes and brought to the surface (9 total samples). On the surface, the boat crew immediately filtered 100 mL of sample through lab-rinsed GF/C filters into single-use poly bottles which were stored in the dark on ice until returning to the lab. Samples were frozen at -20°C until shipment was made to NWQR. NCWQR analyzed samples for seven constituents: ammonia (NH_3), chloride (Cl^-), sulfate (SO_4^-), nitrite (NO_2), nitrate (NO_3), silicon dioxide (SiO_2), and soluble reactive phosphorous (SRP).

Benthic Cladophora and mussel collections

Divers collected replicate ($n = 5$), 0.25 m^2 quadrat air-lift samples on each sample date and depth to quantify benthic algal biomass and dreissenid abundance. Divers placed quadrats haphazardly on the lake bottom and airlifted all material within the quadrat into large mesh bags (0.5 mm mesh) attached to the air-lift tube. Samples bags were taken to the surface and stored on ice in the dark until returning to the lab. In the lab, samples were gently washed over a sieve series to remove mud and silt. Samples were then hand-picked to remove algae attached to mussels or floating in a shallow tray. The entire algal collection was wet-weighed by placing between layers of paper towel and applying pressure to remove as much water as possible prior to obtaining the mass. From this mass, several subsamples were removed and processed for either chlorophyll a , dry mass, CN ratio, or P content. All mussels and invertebrates were preserved for other studies and not reported here.

Findings

Profiles

Profiles of various parameters indicated that the nearshore zone under study in this 90-day project was well-mixed.

Temperature and dissolved oxygen Surface and bottom temperature data suggest a well-mixed nearshore environment. On each sampling date, surface and bottom temperatures were generally

within 3° C of each other (Fig. 2a). At least 2 upwelling events, when water temperature declined by at least 4° C, were observed during the 90-day sampling period. More frequent temperature recordings from bottom-moored temperature loggers showed a much more dynamic temperature regime in the nearshore, with at least 5 upwelling events recorded (Fig 2b). On all sample dates and depths, dissolved oxygen was near or above saturation levels, depending on temperature (90-day mean = 10.7±0.59 mg/L (se)).

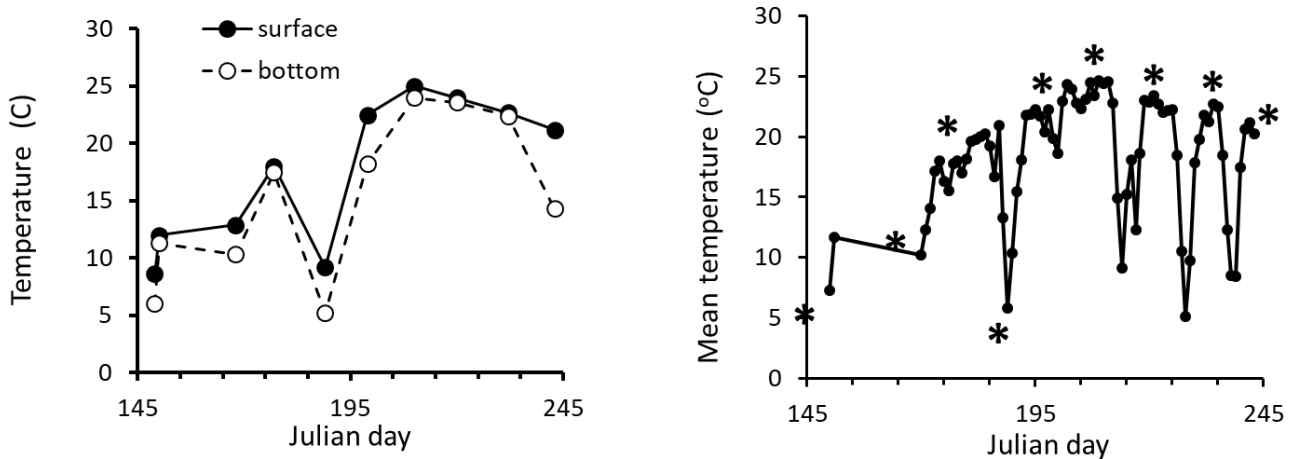


Figure 2. Surface and bottom temperature (A) and average bottom temperature over 90-day sampling period (B). Asterisks in B represent dates divers collected samples and dates for surface profiles.

Light penetration %PAR) and Secchi disc Light penetration profiles suggested ample light for *Cladophora* growth reached the bottom on most sampling dates (Fig. 3). In general, light at the bottom over the 6 and 3 meter contours exceeded 20% of surface PAR, and % PAR at 9 meters rarely was less than 10%. Secchi disc depths were in good agreement with light transmission observations from the PAR sensor. Over the sampling period, Secchi disc depth averaged 6 meters, with a maximum reading of 8.2 m (Fig. 4). The light profile data correlated well with Secchi disc depth ($r = 0.83$, $P = 0.006$).

Conductivity Conductivity profiles showed no changes from surface to bottom and mean values did not differ across sampling dates ($F_{8,90} = 1.02$; $P = 0.424$). Conductivity averaged 297 mS/cm over the summer of collections.

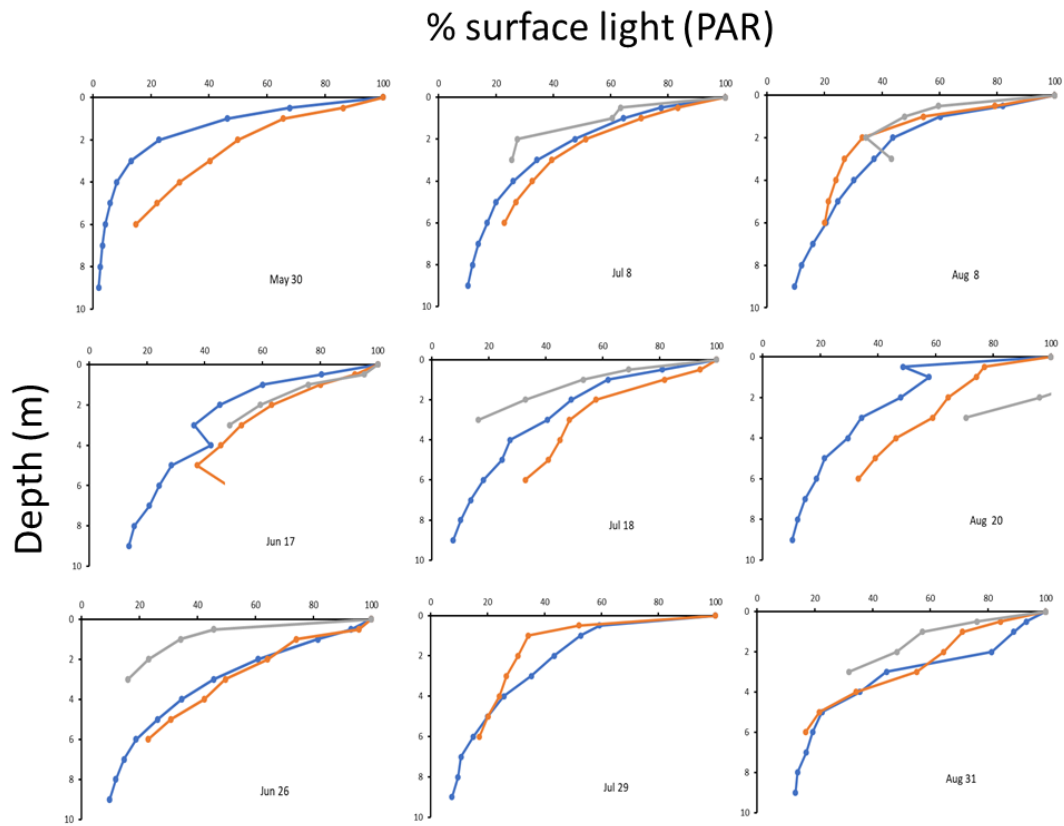


Figure 3. Percent surface PAR on each sampling date. Blue lines = 9m. Orange lines = 6 m. Grey lines = 3 m.

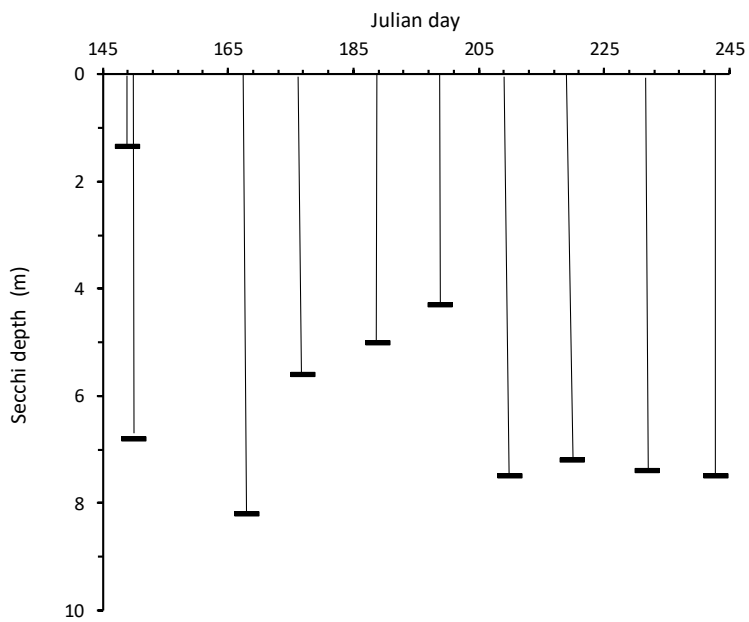


Figure 4. Secchi disc depth on each sampling date.

Nutrient chemistry Water column nutrients, like the profile observations, also suggested a well-mixed nearshore zone, but with a few differences. Surface water samples were first analyzed for spatial differences, since the depth contours also reflect distance from shore. Data were coded to investigate the effects of upwellings, which occurred on Julian days 150 and 189 of sampling. Additionally, Julian day ($n = 9$) was grouped into seasons (early, mid, and late growing season) in part to reduce df lost to time in ANOVA procedures and to reflect *Cladophora* growth dynamics. Over the sampling period, no surface nutrient showed a significant differences across depths (all $P > 0.05$; Appendix B for full ANOVA outputs), thus distance from shore did not affect surface water nutrient concentrations.

Both season and upwelling occurrence had some effect on surface nutrients. Both SRP and TIN declined with season (Appendix B). SRP showed a consistent decline with season, except for a local increase in concentration on upwelling dates (Fig. 5a) and total inorganic nitrogen (TIN) showed a seasonal decline but slight increases on the tail end of a midsummer upwelling (Fig. 5b). Only surface SRP was affected by the occurrence of upwellings, exhibiting higher concentrations on upwelling days relative to non-upwelling days (Fig 5a; Appendix B; $F_{1,11} = 25.76$, $P < 0.001$).

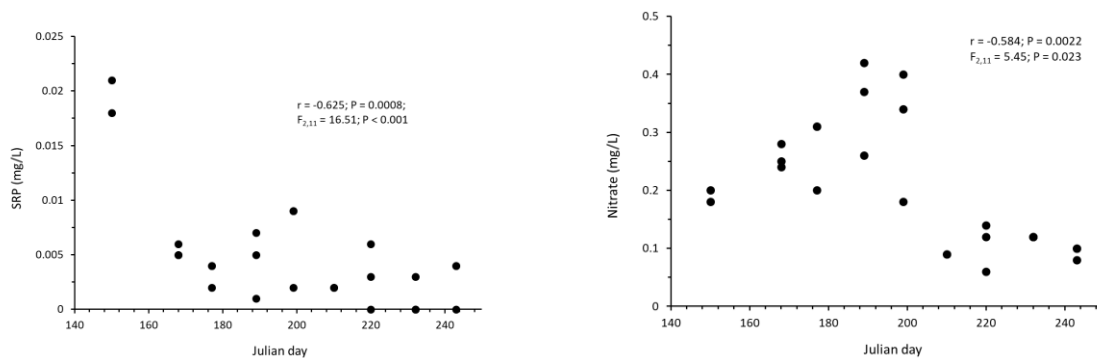


Figure 5. Surface water SRP (A) and TIN (B) concentrations over the 90-day sampling period.

Surface waters were next compared to bottom waters on each sampling date within each depth. In this analysis, surface point samples were compared to the ‘upcurrent’ collections of bottom water to eliminate direct influence of mussel and *Cladophora* patches on comparisons. Like the surface spatial pattern of no difference, surface and bottom waters at 3, 6, and 9 meter locations did not differ over the sampling period (all $P > 0.05$). SRP, chloride, and sulfate concentrations approached significance ($P = 0.072$, 0.077 , and 0.093 , respectively), possibly reflecting an upwelling effect.

Microscale nutrient responses to *Cladophora*/*Dreissena* assemblages There was no observable change in bottom nutrient concentrations (e.g., TIN, SO_4 , SRP, Cl, or SiO_2) as a water mass passed over and past a mussel/*Cladophora* assemblage (all ‘Location’ effects $P > 0.05$). Even when analyses were restricted to just the 6-m depth collections (since this depth zone was sampled on all dates) there was not a significant ‘location’ effect for any nutrient (all $P > 0.05$). However, within-site and across season variability matched or exceeded within-assemblage variability in SRP, nitrate, and ammonia concentrations, making it difficult to evaluate microscale nutrient changes. A broader-stroke inspection of these nutrients suggested both nitrate and ammonia levels decreased more often than expected by chance ($G_{adj} = 6.25$ and 17.71 ; $P = 0.044$ and < 0.001 , respectively), whereas SRP levels declined, increased, or remained unchanged as would be expected by chance ($G_{adj} = 4.438$, $P = 0.109$). Thus, at the

microscale level sampled in this study, it appears that nutrient release/uptake from mussel/*Cladophora* assemblages, when present at the densities or biomass observed during summer 2019, have little discernible effects on water column nutrients.

Bottom water nutrients and upwellings Unlike surface waters, there were some spatial differences in bottom water nutrient concentrations. Both silicon dioxide and SRP levels increased with depth (Appendix C: $F_{2,60} = 3.69$ and 10.49 ; $P = 0.031$ and <0.001 , respectively). All nutrients responded to season and upwelling occurrence (Appendix C). Constituents generally declined with season and increased with upwelling occurrence. The ‘season*upwelling’ interaction also was significant for all bottom nutrients, making interpretation of main effects a bit more difficult. However, since upwellings only occurred during our early season sampling dates, these two variables exhibit high collinearity. The most difficult nutrient to interpret was SRP since every 2-way and 3-way interaction was significant in the analysis (Appendix C).

Cladophora growth and coverage During the summer 2019 growing season, the collection area near Olcott, NY had roughly 35% *Cladophora* coverage over the sampling period with considerable variability. This is in good agreement with the Brooks et al. (2015) estimate of 40% coverage for the Lake Ontario nearshore observed with Landsat imagery. The 9-m sample sites consistently had the least algae, whereas the 6- and 3-m depths had higher coverage estimates (Fig. 6). Mean coverage by depth was 39, 59, and 5% for the 3, 6, and 9 meter depths. Coverage was strongly correlated with percent cobble substrate where random collections were made ($r = 0.55$, $P = 0.007$; Fig. 7). In addition to *Cladophora*, mid and late summer explosions of *Spirogyra* were observed by divers throughout the 6 and 3 meter locations, but not quantified.

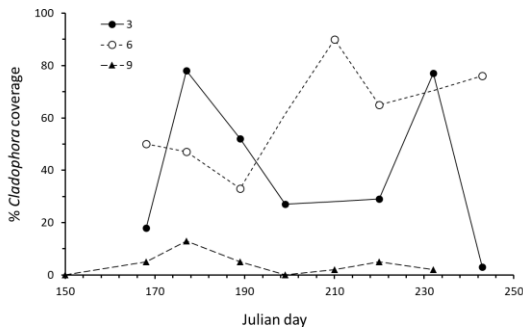


Figure 6. *Cladophora* coverage thru time.

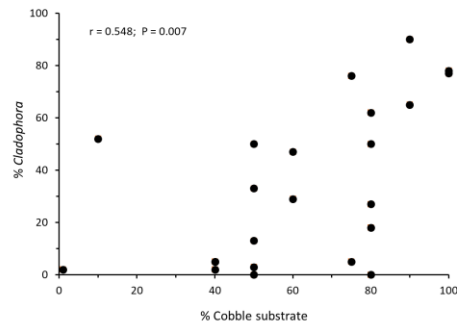


Figure 7. Relationship between *Cladophora* percent coverage and percent cobble substrate.

Cladophora biomass exhibited increasing growth through the end of July, on average, before declining in abundance (Fig. 8). The pattern differed by depth. There was still substantial biomass collected at the 3-m depth stations into the middle of August. Biomass declined with season (Appendix D; $F_{2,45} = 5.51$, $P = 0.007$) and declined with depth ($F_{2,45} = 10.07$, $P < 0.001$). Although biomass occasionally exceeded the general ‘rule-of-thumb’ for nuisance levels (50 mg/m^2), on most dates and depths it was below nuisance levels. Similarly, although the growth pattern suggested maximum

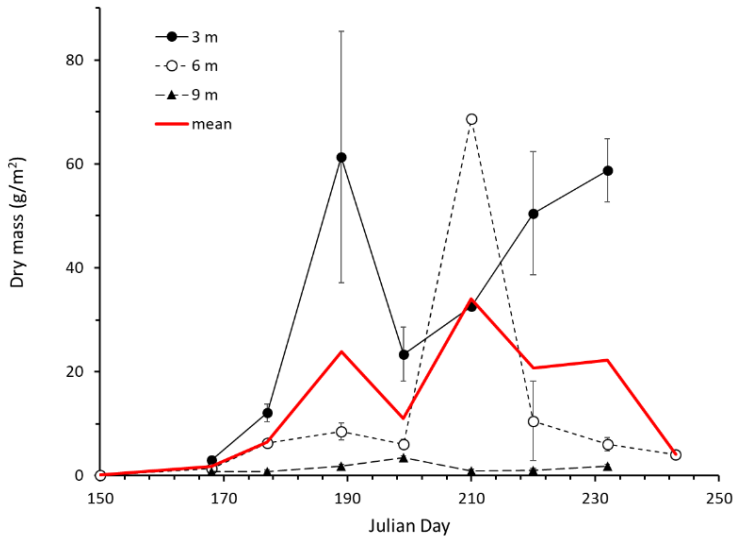


Figure 8. Mean biomass of *Cladophora* at the Olcott sampling site in summer 2019. Error bars are 1 s.e.

biomass up until the end of July, followed by a decrease, we did not observe a robust sloughing event. Nor was there evidence of shoreline windrows of algal mats through our sampling window.

The overall appearance and nutrient condition of *Cladophora* stands showed marked changes through the sampling season and with depth. Stand ash-free dry mass (AFDM) is a good reflection of organic matter content, and this value declined through the sampling season (Fig. 9). Visually, *Cladophora* stands got ‘duller’ through the season as they began to both senesce and become covered with layers of silt.

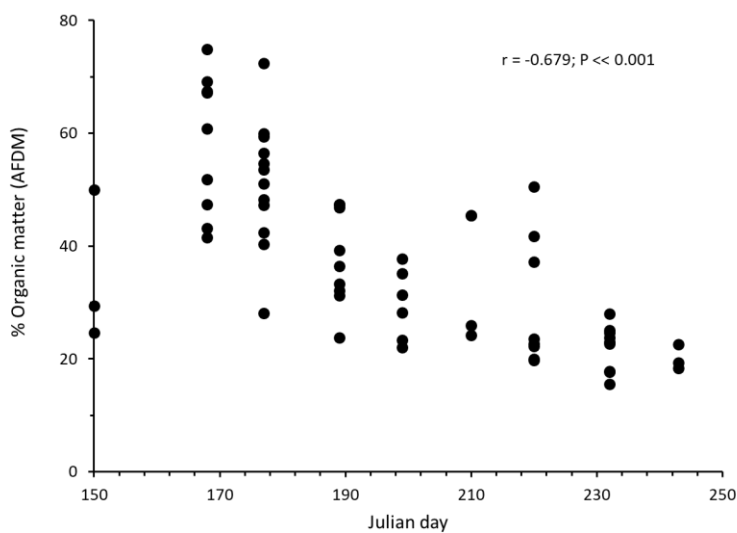


Figure 9. Percent organic matter of *Cladophora* stands through the summer, 2019.

Nutrient content of *Cladophora* tissue may provide some evidence as to when a sloughing event might occur, since senescing tissues invest less in pigment production and starch storage. It is generally believed that *Cladophora* requires a minimum tissue P level of 0.035 to 0.06% is needed for growth (Auer and Canale 1982, Tomlinson et al. 2010) and levels below 0.1% indicate P-limitation (Auer and Canale 1982). Tissue P levels were fairly consistent throughout the 2019 growing season in this region of Lake Ontario, and indicated a season-long, P-limitation (season average = 0.048 ± 0.004 (s.e.)).

Carbon, nitrogen, phosphorous, and chlorophyll *a* content were all lowest at 3-m stations and highest at 9-m stations over the sampling season (Appendix E; all $P < 0.05$). This pattern might suggest a higher pigment investment under low light conditions (e.g., Falkowski and LaRoche 1991). The C:N ratio pattern across depth followed from the individual C and N levels, resulting in the highest C:N at the 3 m site and the lowest C:N at the 9 m sites. Similarly, tissue nutrients exhibited consistent patterns through the season. Nitrogen, carbon, and chlorophyll *a* content all declined with season (Appendix E; all $P < 0.05$), whereas P levels in tissue remained constant. This makes some sense since the chlorophyll molecule is carbon and nitrogen rich, but contains no P. Chlorophyll content also responded to an upwelling event in early July (Fig. 10), exhibiting a sharp decline. Although there was a season long trend in a chlorophyll reduction, this particular day was the only day to differ significantly from both the preceding and following sampling days ($t = 4.26$ and 2.22 ; $P < 0.001$ and $P = 0.039$, respectively). Low temperature exposure ought to limit carbon fixation in algae, which, if light levels remain unchanged, should reduce its ability to photosynthesize (Davison 1991). Each of these main effects (depth, season, and upwelling occurrence), although having significant effects on the nutrients considered, also had a number of significant interaction terms making them more difficult to decipher. Additionally, since *Cladophora* samples were only collected during a single upwelling occurrence in season 2 (July 8), all interaction terms with 'upwelling' and 'season' are uninterpretable due to lack of variance.

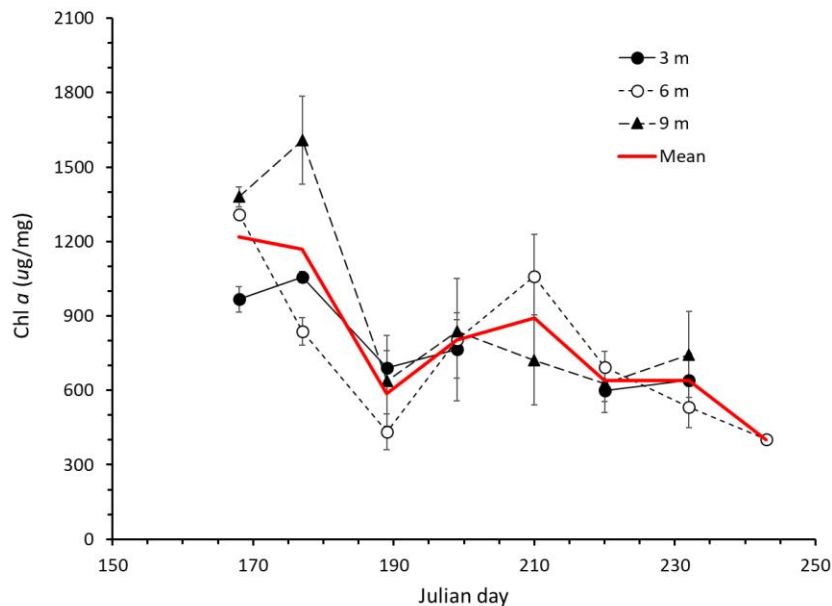


Figure 10. Chlorophyll *a* content in *Cladophora* tissue over the sampling period in summer 2019. An upwelling event occurred on day 189 (July 8).

***Dreissena* population update** Across all date/depth combinations, the mean *Dreissena* density, inclusive of juveniles, was 3337 mussels/m² (\pm 675 s.e.; min = 0, max = 32,000). Both depth and date were important in determining the mean number of non-juvenile mussels observed (>5 mm) (Appendix E). For depth, more non-juvenile mussels were observed at 6 m than either 3 or 9 m, and fewer were observed at 3 m than 9 m (Fig. 11). Across seasons, more non-juvenile mussels were observed later in the year than during the first month (Fig. 11), suggesting rapid mass accrual during the sampling season. Conversely, juveniles (<5 mm) did not show any seasonal pattern, comprising about 55.5% of the counts across seasons, and suggesting spawning occurred throughout the sampling season. There appeared to be somewhat better juvenile recruitment in deeper waters (e.g., 62% vs 49% average across all dates; $F_{2,58} = 3.51$, $P = 0.043$).

Percent composition by juveniles and percent non-juvenile mussels both correlated with *Cladophora* DM, though in opposite directions. Algal DM increased with increasing juvenile proportion ($r = 0.52$, $P < 0.001$), but decreased with adult mussel proportion ($r = -0.46$, $P = 0.001$). However, both of these correlations likely reflect the coincident changes observed in both algal DM and mussel metrics with depth, since depth was a strong predictor of mussel and algal abundance. Neither total mussel count nor total mussel biomass correlated with *Cladophora* DM (all $P > 0.05$).

Combining mussels, water column nutrients, and environmental conditions The summer 2019 growing season did not produce nuisance *Cladophora* levels in this region of Lake Ontario, even though there was ample substrate for attachment and abundant sunlight for photosynthesis. Conversely, SRP levels were very low (with the exception on an upwelling day) and tissue P data suggested the *Cladophora* in this region was P-limited the entire growing season even though tissue P levels were high enough for growth. A model-building exercise using 15 available variables (Julian day, depth, water temperature, tissue P, tissue C, tissue N, tissue C:N ratio, SRP, TIN, season, *Dreissena* count, *Dreissena* biomass, organic matter content, chlorophyll a content, and upwelling occurrence) to estimate *Cladophora* biomass resulted in a most-parsimonious model including 3 variables: depth, Julian day, and SRP. That model was $DM (g/m^2) = -0.306(\text{depth}) - 357.83(\text{SRP} + 0.011(\text{Julian}))$. This model explained almost 70% of the variability in *Cladophora* dry mass ($R^2 = 0.695$; $F_{3,45} = 34.24$, $P < 0.001$).

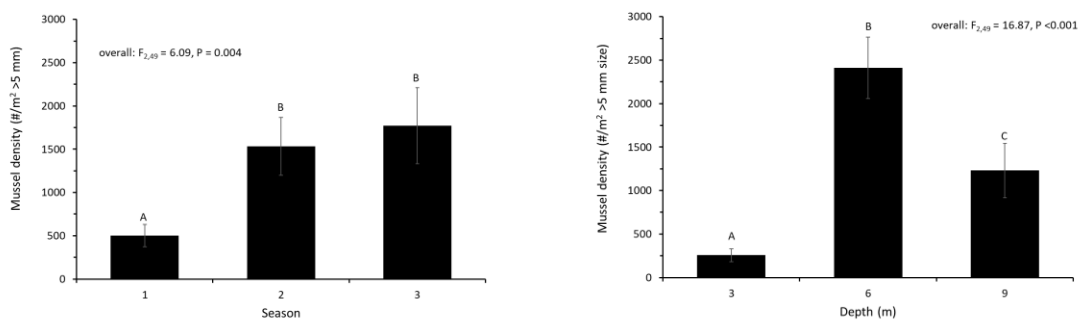


Figure 11. Density of non-larval *Dreissena* (>5 mm) relative to season and depth in nearshore Lake Ontario.

Nearshore data combined with satellite imagery The nearshore *Cladophora* summary information and temperature and light profile data (percent cover, chl *a* content, temperature, PAR, Secchi disc depth) were shared with collaborators at Michigan Technological Institute to help improve interpretation of available imagery and recommend adjustments to the *Cladophora* Growth Model.

As part of that imagery assessment, collaborators determined that the percent cover by *Cladophora* in our study area has remained fairly stable at approximately 60% since the mid 1970's, even though the total mappable area has almost doubled due to increased light penetration (MTRI 2020). Although the nearshore imagery performed by MTRI suggests submerged aquatic vegetation (SAV) as the source of their spectral signatures and they suggest it is 'mostly' *Cladophora*, our observations suggest other benthic algae may contribute substantially to that spectral signature (e.g., *Spirogyra*), especially late in the season. For the 2019 growing season, only 5 satellite images over the sampling area were usable due to cloud cover or concordance with actual sampling dates. The 2019 images corroborate the mean biomass and coverage field data as having midsummer peaks and then a decline and 'heat maps' of *Cladophora* coverage provide excellent matches on 6 possible corroboration points (day by depth possibilities) (MTRI 2020). The full MTRI technical report can be found in Appendix F.

Outputs Several outreach deliverables have been and are being prepared from this seasonal effort. Three presentations have been accepted for the 2020 IAGLR conference being held in Winnipeg, Manitoba in June (Appendix F for titles and abstracts). The Pennuto lab is preparing two manuscripts to be included in a special CSMI edition of the Journal of Great Lakes Research and MTRI collaborators are preparing a third manuscript resulting from this work.

Fiscal summary The final accounting for this award showed an ending balance of approximately \$754 (Appendix H).

Literature Cited

- American Public Health Association (APHA). 1998. Standard methods for the examination of water and wastewater, 20th ed. United Books Press.
- Auer MT, Kuczynski A, and Gawde RK. 2014. Phosphorus provenance and *Cladophora* growth in Lake Ontario. Final Report, October, 2014. https://www.ajax.ca/en/livinginajax/resources/duffin-creek-wpcp/documents/Phosphorus_Provenance_Final_Report_24_Oct_2014.pdf
- Auer MT and Canale RP. 1982. Ecological studies and mathematical modeling of *Cladophora* in Lake Huron: 3. The dependence of growth rates on internal phosphorous pool size. *Journal of Great Lakes Research* 8:93-99.
- Bootsma HA, Rowe MD, Brooks CN, and Vanderploeg HA. 2015. Commentary: the need for model development related to *Cladophora* and nutrient management in Lake Michigan. *Journal of Great Lakes Research* 41 (Supplement 3):7-15.
- Brooks C, Grimm A, Shuchman R, Sayers M, and Nathaniel J. 2015. A satellite-based multi-temporal assessment of the extent of nuisance *Cladophora* and related submerged aquatic vegetation for the Laurentian Great Lakes. *Remote Sensing of Environment* 157:58-71.
- Davison IR. 1991. Environmental effects on algal photosynthesis: temperature. *Journal of Phycology* 27:2-8.
- Dayton AI, Auer MT, and Atkinson JF. 2014. *Cladophora*, mass transport, and the nearshore phosphorous shunt. *Journal of Great Lakes Research* 40:790-799.
- Dove A and Chapra SC. 2015. Long-term trends of nutrients and trophic response variables for the Great Lakes. *Limnology and Oceanography* 60:696-721.
- Falkowski G and LaRoche J. 1991. Acclimation to spectral irradiance in algae. *Journal of Phycology* 27:8-14.
- Higgins SN, Hecky RE, and Guilford SJ. 2005. Modeling the growth, biomass, and tissue phosphorus concentration of *Cladophora glomerata* in eastern Lake Erie: model description and field testing. *Journal of Great Lakes Research* 31:439-455.
- Higgins SN, Pennuto CM, Howell ET, Lewis TW, and Makarewicz JC. 2012. Urban influences on *Cladophora* blooms in Lake Ontario. *Journal of Great Lakes Research* 38(Suppl. 4):116-123.
- Howell ET and Dove A. 2017. Chronic nutrient loading from Lake Erie affecting water quality and nuisance algae on the St. Catherine's shores of Lake Ontario. *Journal of Great Lakes Research* 43:899-915.
- Kuczynski A., Auer MT, Brooks CN, and Grimm AG. 2016. The *Cladophora* resurgence in Lake Ontario: characterization and implications for management. *Canadian Journal of Fisheries and Aquatic Sciences* 73:999-1013.
- Makarewicz JC, Lewis TW, Pennuto CM, Atkinson JF, Edwards WJ, Boyer GL, Howell ET, and Thomas G. 2012. Physical and chemical characteristics of the nearshore zone of Lake Ontario. *Journal of Great Lakes Research* 38(Suppl. 4):21-31.
- Michigan Technological Research Institute (MTRI). 2020. Combining *in situ* Lake Ontario measurements of *Cladophora* with satellite-derived observations for improved assessments. MTRI Technical Report, January 2020.
- Ozersky, T, Malkin SY, Barton DR, and Hecky RE. 2009. Dreissenid phosphorous excretion can sustain *C. glomerata* growth along a portion of Lake Ontario shoreline. *Journal of Great Lakes Research*. 35:321-328.
- Pennuto CM, Howell ET, and Makarewicz JC. 2012. Relationships among round gobies, *Dreissena* mussels, and benthic algae in the south nearshore of Lake Ontario. *Journal of Great Lakes Research*. 38(Suppl. 4):154-160.

- Pennuto CM, Howell ET, Lewis TW, and Makarewicz JC. 2012. *Dreissena* population status in nearshore Lake Ontario. *Journal of Great Lakes Research*. 38(Suppl. 4):161-170.
- Redder T, Peterson G, and Atkinson J. 2017. Preliminary recommendations for Lake Ontario CSMI monitoring components to support lake water quality and ecosystem modeling for Annex 4. LimnoTech Memorandum to Fred Luckey, USEPA. May 2017.
- Steinman AD, Lamberti GA, Leavitt PR. 2007. Biomass and pigments of benthic algae. In Hauer FR, Lamberti GA (eds), *Methods in stream ecology*, 2nd edn. Academic Press, pp 357-379.
- Tomlinson LM, Auer MT, Bootsma HA, and Owens EM. 2010. The Great Lakes *Cladophora* model: development, testing and application to Lake Michigan. *Journal of Great Lakes Research* 36:287-297.
- Watkins JM, Weidel BC, Fisk AT, and Rudstam LG. 2017. Cooperative science to inform Lake Ontario management: research from the 2013 Lake Ontario CSMI program. *Journal of Great Lakes Research* 43:779-781.
- Weber CI. 1973. Biological field and laboratory methods for measuring the quality of surface waters and effluents. U.S. Environmental Protection Agency Report 670 / 4 / 73 / 001.

Appendix A. Surface nutrient chemistry ANOVA outputs.

Dependent Variable: SO4

Source	Type III Sum of Squares	df	Mean Square	F	Sig.
Depth	42.647	2	21.323	.985	.404
Season	91.673	2	45.836	2.117	.167
Upwell	70.290	1	70.290	3.247	.099
depth * season	183.389	4	45.847	2.118	.147
depth * upwell	145.536	2	72.768	3.361	.073
season * upwell	4.420	1	4.420	.204	.660
depth * season * upwell	52.510	1	52.510	2.426	.148
Error	238.125	11	21.648		
Total	9299.010	25			

Dependent Variable: CL

Source	Type III Sum of Squares	df	Mean Square	F	Sig.
depth	53.842	2	26.921	1.220	.332
season	53.719	2	26.859	1.217	.333
upwell	71.918	1	71.918	3.260	.098
depth * season	120.866	4	30.217	1.370	.306
depth * upwell	97.198	2	48.599	2.203	.157
season * upwell	.167	1	.167	.008	.932
depth * season * upwell	23.602	1	23.602	1.070	.323
Error	242.683	11	22.062		
Total	10555.730	25			

Appendix A continued

Dependent Variable: SRP

Source	Type III Sum of Squares	df	Mean Square	F	Sig.
depth	3.407E-6	2	1.703E-6	.270	.768
season	.000	2	.000	16.505	.000
upwell	.000	1	.000	25.775	.000
depth * season	1.830E-5	4	4.576E-6	.726	.592
depth * upwell	2.050E-5	2	1.025E-5	1.626	.241
season * upwell	.000	1	.000	33.324	.000
depth * season * upwell	1.204E-5	1	1.204E-5	1.910	.194
Error	6.933E-5	11	6.303E-6		
Total	.001	25			

Dependent Variable: TIN

Source	Type III Sum of Squares	df	Mean Square	F	Sig.
depth	.016	2	.008	.833	.460
season	.102	2	.051	5.459	.023
upwell	.011	1	.011	1.158	.305
depth * season	.013	4	.003	.357	.834
depth * upwell	.006	2	.003	.299	.747
season * upwell	.023	1	.023	2.452	.146
depth * season * upwell	.012	1	.012	1.232	.291
Error	.103	11	.009		
Total	1.733	25			

Appendix A continued.

Dependent Variable: SiO2

Source	Type III Sum of Squares	df	Mean Square	F	Sig.
depth	.012	2	.006	.183	.835
season	.008	2	.004	.125	.884
upwell	.057	1	.057	1.718	.217
depth * season	.045	4	.011	.341	.845
depth * upwell	.025	2	.013	.385	.689
season * upwell	.099	1	.099	2.997	.111
depth * season * upwell	.018	1	.018	.550	.474
Error	.363	11	.033		
Total	4.776	25			

Appendix B. Bottom nutrient chemistry ANOVA outputs.

Dependent Variable: chloride

Source	Type III Sum of Squares	df	Mean Square	F	Sig.
depth	22.788	2	11.394	.767	.469
season	101.783	2	50.892	3.426	.039
upwelling	77.170	1	77.170	5.196	.026
depth * season	25.787	4	6.447	.434	.783
depth * upwelling	46.896	2	23.448	1.579	.215
season * upwelling	170.571	1	170.571	11.484	.001
depth * season * upwelling	64.027	1	64.027	4.311	.042
Error	891.160	60	14.853		
Total	28341.020	74			

Dependent Variable: sulfate

Source	Type III Sum of Squares	df	Mean Square	F	Sig.
depth	26.809	2	13.404	.828	.442
season	199.728	2	99.864	6.168	.004
upwelling	65.129	1	65.129	4.023	.049
depth * season	36.069	4	9.017	.557	.695
depth * upwelling	74.705	2	37.353	2.307	.108
season * upwelling	100.616	1	100.616	6.214	.015
depth * season * upwelling	94.521	1	94.521	5.838	.019
Error	971.456	60	16.191		
Total	25021.740	74			

Appendix B continued.

Dependent Variable: silicon

Source	Type III Sum of Squares	df	Mean Square	F	Sig.
depth	.165	2	.083	3.691	.031
season	.479	2	.239	10.691	.000
upwelling	.437	1	.437	19.504	.000
depth * season	.049	4	.012	.548	.701
depth * upwelling	.212	2	.106	4.737	.012
season * upwelling	1.407	1	1.407	62.809	.000
depth * season * upwelling	.024	1	.024	1.050	.310
Error	1.344	60	.022		
Total	18.254	74			

Dependent Variable: SRP

Source	Type III Sum of Squares	df	Mean Square	F	Sig.
depth	.000	2	5.232E-5	10.498	.000
season	.000	2	5.835E-5	11.710	.000
upwelling	8.928E-5	1	8.928E-5	17.916	.000
depth * season	7.662E-5	4	1.915E-5	3.844	.008
depth * upwelling	9.942E-5	2	4.971E-5	9.975	.000
season * upwelling	3.984E-5	1	3.984E-5	7.994	.006
depth * season * upwelling	3.694E-5	1	3.694E-5	7.413	.008
Error	.000	60	4.983E-6		
Total	.002	74			

Appendix B continued.

Dependent Variable: TIN

Source	Type III Sum of Squares	df	Mean Square	F	Sig.
depth	.005	2	.003	.519	.598
season	.241	2	.120	24.333	.000
upwelling	.031	1	.031	6.254	.015
depth * season	.013	4	.003	.650	.629
depth * upwelling	.019	2	.009	1.920	.156
season * upwelling	.187	1	.187	37.895	.000
depth * season * upwelling	.016	1	.016	3.231	.077
Error	.297	60	.005		
Total	4.600	74			

Appendix C. *Cladophora* biomass ANOVA results examining season and depth effects.

Dependent Variable: DryMass

Source	Type III Sum of Squares	df	Mean Square	F	Sig.
depth	5533.305	2	2766.652	10.065	.000
season	3030.311	2	1515.156	5.512	.007
depth * season	3432.670	4	858.167	3.122	.024
Error	12369.562	45	274.879		
Total	37829.472	54			

Appendix D. ANOVA outputs examining depth, season, and upwelling effects on *Cladophora* tissue nutrients.

Dependent Variable: Percent N

Source	Type III Sum of Squares	df	Mean Square	F	Sig.
Depth	124.370	2	62.185	73.278	.000
season	174.875	2	87.438	103.036	.000
upwelling	4.342	1	4.342	5.116	.025
Depth * season	57.396	4	14.349	16.909	.000
Depth * upwelling	8.851	2	4.425	5.215	.006
season * upwelling	.000	0	.	.	.
Depth * season * upwelling	.000	0	.	.	.
Error	132.383	156	.849		
Total	1821.891	168			

Dependent Variable: Percent C

Source	Type III Sum of Squares	df	Mean Square	F	Sig.
Depth	628.967	2	314.483	28.013	.000
season	5040.390	2	2520.195	224.489	.000
upwelling	120.039	1	120.039	10.693	.001
Depth * season	317.485	4	79.371	7.070	.000
Depth * upwelling	14.140	2	7.070	.630	.534
season * upwelling	.000	0	.	.	.
Depth * season * upwelling	.000	0	.	.	.
Error	1751.314	156	11.226		
Total	71096.184	168			

Dependent Variable: C:N ratio

Source	Type III Sum of Squares	df	Mean Square	F	Sig.
Depth	687.577	2	343.789	183.129	.000
season	61.095	2	30.547	16.272	.000
upwelling	.058	1	.058	.031	.861
Depth * season	122.885	4	30.721	16.365	.000
Depth * upwelling	66.324	2	33.162	17.665	.000
season * upwelling	.000	0	.	.	.
Depth * season * upwelling	.000	0	.	.	.
Error	292.860	156	1.877		
Total	16501.731	168			

Appendix D continued.

Dependent Variable: Percent P

Source	Type III Sum of Squares	df	Mean Square	F	Sig.
depth	.030	2	.015	4.662	.015
season	.006	2	.003	.944	.397
upwelling	.000	1	.000	.100	.754
depth * season	.018	4	.004	1.358	.264
depth * upwelling	.017	1	.017	5.294	.026
season * upwelling	.000	0	.	.	.
depth * season * upwelling	.000	0	.	.	.
Error	.143	44	.003		
Total	.691	55			

Dependent Variable: Chlorophyll a content

Source	Type III Sum of Squares	df	Mean Square	F	Sig.
depth	393621.659	2	196810.830	4.348	.017
season	3454524.507	2	1727262.254	38.163	.000
upwelling	432444.069	1	432444.069	9.555	.003
depth * season	902275.683	4	225568.921	4.984	.001
depth * upwelling	356302.810	2	178151.405	3.936	.024
season * upwelling	.000	0	.	.	.
depth * season * upwelling	.000	0	.	.	.
Error	3032398.536	67	45259.680		
Total	68582913.820	79			

Appendix E. ANOVA outputs examining season and depth effects on *Dreissena* metrics.

Source	Dependent Variable	Type III Sum of Squares	df	Mean Square	F	Sig.
season	Musselcount	14403371.030	2	7201685.516	6.093	.004
	Arcsinpercent	.551	2	.275	2.161	.126
depth	Musselcount	39871112.930	2	19935556.460	16.866	.000
	Arcsinpercent	.453	2	.227	1.778	.180
season * depth	Musselcount	10201328.340	4	2550332.084	2.158	.088
	Arcsinpercent	1.683	4	.421	3.302	.018
Error	Musselcount	57916618.220	49	1181971.800		
	Arcsinpercent	6.244	49	.127		
Total	Musselcount	221413324.700	58			
	Arcsinpercent	23.023	58			

Appendix F. Titles and abstracts for presentations to be given at the 2020 IAGLR conference in Winnipeg, Manitoba using data generated during the 2019 field season on *Cladophora* dynamics.

1) *Cladophora* and mussel dynamics in nearshore Lake Ontario: a contrary observation.

James Wagner and Christopher M. Pennuto, Biology Department, Buffalo State College

Non-native dreissenid mussels are implicated in the resurgence of nuisance *Cladophora* mats. However, not all regions of the Great Lakes with high dreissenid numbers, with significant light penetration, or with bioavailable phosphorous have nuisance *Cladophora*. We examined mussel abundance and biomass, *Cladophora* biomass, mussel and algal tissue nutrient conditions, and water column nutrients in the nearshore of southwest Lake Ontario over a 90-day algal growth season. Neither mussel biomass nor abundance (#/m²) correlated with *Cladophora* biomass over the sampling days or within a depth zone. Both mussel metrics and *Cladophora* biomass were influenced by depth; positively for mussels and negatively for algae. *Cladophora* tissue P was unrelated to mussel abundance or water column SRP. Collectively, these patterns suggest that either other factors are critical to the creation of nuisance *Cladophora* mats in Lake Ontario, or the usual triad of needed resources (i.e., SRP, light, and substrate) interact in as yet misunderstood ways. Alternatively, mat occurrence and magnitude may simply be dictated by local conditions not present in the current sampling area.

2) *Cladophora* nutrient and chlorophyll status responds to abiotic conditions in Lake Ontario.

Christopher M. Pennuto and James Wagner, Biology Department, Buffalo State College.

Beach fouling and waterworks impacts from sloughed *Cladophora* mats pose a nuisance in several Great Lakes. We documented microscale nutrient conditions in and around *Cladophora* mats at three depths (3, 6, 9 meter), as well as internal chlorophyll and nutrient levels through the 2019 growing season in SW Lake Ontario. *Cladophora* mat biomass peaked in late July but was greatest at the shallowest depth, and occasionally exceeded nuisance levels. No obvious sloughing event was observed. Water column SRP, and NH₃ levels were controlled by season and depth, but also exhibited changes as water passed through/over *Cladophora*-dreissenid assemblages. Chlorophyll content was affected by date and depth, declining with season and upwelling, but increasing with depth. Tissue P levels were greater with depth even though water column P level were not different. Upwelling events affected water column SRP, NO₃, and NH₃ concentration throughout the study area. These observations collectively suggest *Cladophora* abundance in this area of Lake Ontario was below nuisance levels and that tissue chlorophyll, but not nutrient content, were affected by upwelling occurrence.

3) Annual *Cladophora* extent monitoring with moderate resolution satellites at 12 sentinel locations

Amanda Grimm, Robert Shuchman, Mike Sayers, and Sawtell, Michigan Technological Research Institute

Benthic vegetation along many open coastlines of the lower four Laurentian Great Lakes is dominated by *Cladophora*, a prolific native alga. Combining data from Landsat 8 and Sentinel-2, which was launched in 2015 and has Landsat-like bands, provides more frequent imaging for timely monitoring. We assembled time series of imagery for three sites in each of the lower four Great Lakes. Imagery was processed and classified using a semi-automated approach that utilizes a novel depth-invariant method. These time series document the *Cladophora* resurgence in the wake of the introduction of invasive mussels. The analysis also indicates that the effects of invasive mussels on water clarity, which has continued to increase in some places over the last decade, are enabling *Cladophora* to grow in deeper water than was previously considered possible. This new information on the patterns of *Cladophora* growth will support management efforts and help to prioritize nutrient abatement programs.

Appendix G. Final financial statement from Research Foundation of NY for this award.

Federal Financial Report
(Follow form Instructions)

OMB Number: 4040-0014
Expiration Date: 01/31/2019

1. Federal Agency and Organizational Element to Which Report is Submitted US Geological Survey		2. Federal Grant or Other Identifying Number Assigned by Federal Agency (To report multiple grants, use FFR Attachment) G18AC00329	
3. Recipient Organization (Name and complete address including Zip code) Recipient Organization Name: The Research Foundation for SUNY / Buffalo State College Street1: 1300 Elmwood Avenue Street2: City: Buffalo County: Erie State: NY: New York Province: Country: USA: UNITED STATES ZIP / Postal Code: 14222-1095			
4a. DUNS Number 612724732	4b. EIN 14-1368361	5. Recipient Account Number or Identifying Number (To report multiple grants, use FFR Attachment) 82578	
6. Report Type <input type="checkbox"/> Quarterly <input type="checkbox"/> Semi-Annual <input type="checkbox"/> Annual <input checked="" type="checkbox"/> Final	7. Basis of Accounting <input checked="" type="checkbox"/> Cash <input type="checkbox"/> Accrual	8. Project/Grant Period From: 09/01/2018 To: 12/31/2019	9. Reporting Period End Date 12/31/2019
10. Transactions			Cumulative
<i>(Use lines a-c for single or multiple grant reporting)</i>			
Federal Cash (To report multiple grants, also use FFR attachment):			
a. Cash Receipts			100,828.02
b. Cash Disbursements			100,828.02
c. Cash on Hand (line a minus b)			0.00
<i>(Use lines d-o for single grant reporting)</i>			
Federal Expenditures and Unobligated Balance:			
d. Total Federal funds authorized			101,622.00
e. Federal share of expenditures			100,828.02
f. Federal share of unliquidated obligations			0.00
g. Total Federal share (sum of lines e and f)			100,828.02
h. Unobligated balance of Federal Funds (line d minus g)			793.98
Recipient Share:			
i. Total recipient share required			0.00
j. Recipient share of expenditures			0.00
k. Remaining recipient share to be provided (line i minus j)			0.00
Program Income:			
l. Total Federal program income earned			0.00
m. Program Income expended in accordance with the deduction alternative			0.00
n. Program Income expended in accordance with the addition alternative			0.00
o. Unexpended program income (line l minus line m or line n)			0.00

11. Indirect Expense						
a. Type	b. Rate	c. Period From	Period To	d. Base	e. Amount Charged	f. Federal Share
Predetermined	17.50	09/01/2018	12/31/2019	85,811.08	15,016.94	15,016.94
g. Totals:				85,811.08	15,016.94	15,016.94

12. Remarks: Attach any explanations deemed necessary or information required by Federal sponsoring agency in compliance with governing legislation:

13. Certification: By signing this report, I certify to the best of my knowledge and belief that the report is true, complete, and accurate, and the expenditures, disbursements and cash receipts are for the purposes and objectives set forth in the terms and conditions of the Federal award. I am aware that any false, fictitious, or fraudulent information, or the omission of any material fact, may subject me to criminal, civil or administrative penalties for fraud, false statements, false claims or otherwise. (U.S. Code Title 18, Section 1001 and Title 31, Sections 3729-3730 and 3801-3812).

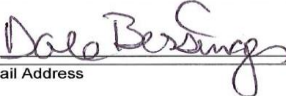
a. Name and Title of Authorized Certifying Official

Prefix: First Name: Middle Name:

Last Name: Suffix:

Title:

b. Signature of Authorized Certifying Official



c. Telephone (Area code, number and extension)

d. Email Address

e. Date Report Submitted

14. Agency use only:



Combining *in situ* Lake Ontario measurements of *Cladophora* with Satellite-Derived Observations for Improved Assessments

Technical Report to support USGS Award to Chris Pennuto, "Support for a Cladophora Growth Model: Frequent Biomass and Coverage Assessments Married to Sentinel 2 Satellite Imagery in Lake Ontario"

January 2020

Table of Contents

Summary	3
Study Site	4
Long-term Annual Time Series	4
Seasonal Time Series for 2018 and 2019	8
Classified Map Validation and Discussion.....	8
Green Reflectance.....	12
Vegetation Indices	13
SAVMA Depth-Invariant Indices.....	14
Discussion	15
References	16

Summary

This report contains the results of the 2019 collaboration between Dr. Chris Pennuto at SUNY Buffalo State and Dr. Robert Shuchman, Dr. Michael Sayers and Amanda Grimm at Michigan Tech Research Institute (MTRI), Michigan Technological University. The overall goal of the collaboration was to further develop the relationships between multispectral satellite data and *Cladophora* distribution in the Great Lakes. The problem was approached by generating both long-term and dense short-term satellite-based time series distribution maps of *Cladophora* and other submerged aquatic vegetation (SAV) of the Buffalo State College study area and comparing the maps to in situ observations of percent cover, biomass and water quality collected over several dates in the 2019 growing season.

The work performed over the period of performance from 1 July 2019- 31 December 2019 included the following specific objectives:

1. Generate an annual SAV extent map from approximately 1975 to present for the Buffalo State College study area. These extent maps, which also indicate changes in water clarity, will be used to better understand the role of invasive species introduction into changes in SAV distribution.
2. Generate seasonal (April-October) SAV distribution and green reflectivity maps for 2018 and 2019. The satellite observations will be compared to the in situ observations to ascertain whether the satellite-derived reflectance products are capable of capturing various stages of *Cladophora* growth. This important data set can also begin to address the question, “can *Cladophora* biomass be estimated from space”? The seasonal analysis will utilize all cloud-free observations from Landsat 8 and Sentinel-2 to produce weekly estimates (assuming clear imagery exists each week).

The long-term time series of classified imagery indicates that the percent cover of *Cladophora* at the study site has remained fairly stable (roughly 2/3 cover) from the mid-1970s to the present, but the surface area of substrate that can be mapped has approximately doubled due to increasing water clarity. This contrasts with the pattern-observed along the Ajax, Ontario shoreline, another time series site on the north side of Lake Ontario, where mappable area has also doubled but where the percentage of lake bottom classified as *Cladophora* has also increased substantially over time. This difference may relate to local drivers such as nutrient sources.

The cloud- and turbidity-free Landsat-8 and Sentinel-2 imagery collected during the 2018 and 2019 growing seasons exhibited a distinct seasonal curve in the percentage of the lake bottom classified as SAV with fairly consistent water clarity. SAVMA indices appeared to be higher during the peak of the growing season and when field-observed percent cover and biomass were higher, whereas green reflectivity was, as expected, lower when percent cover/biomass was higher, and simpler normalized band vegetation indices were less promising. We have begun preparation of a manuscript based on these findings for submission to a refereed journal.

Study Site

Mapping and classification was performed for an approx. 13.4 km stretch of Lake Ontario shoreline between the Tuscarora Bay and Eighteen Mile Creek piers (Fig. 1). This is the same area where Dr. Pennuto collected field data in 2019. Because of its location 35 km east of the mouth of the Niagara River, the site experiences a strong tributary influence, and it is not unusual for a cloud-free satellite image to be unusable for lake bottom mapping due to high nearshore turbidity. This is reflected in the Secchi disk measurements for 2019, which usually ranged between approx. 4 and 8 m but reached as low as 1.35 m on one date in late May. The bottom substrate along this shoreline is mostly hard cobble/bedrock, with fragments of sand and very little mud.

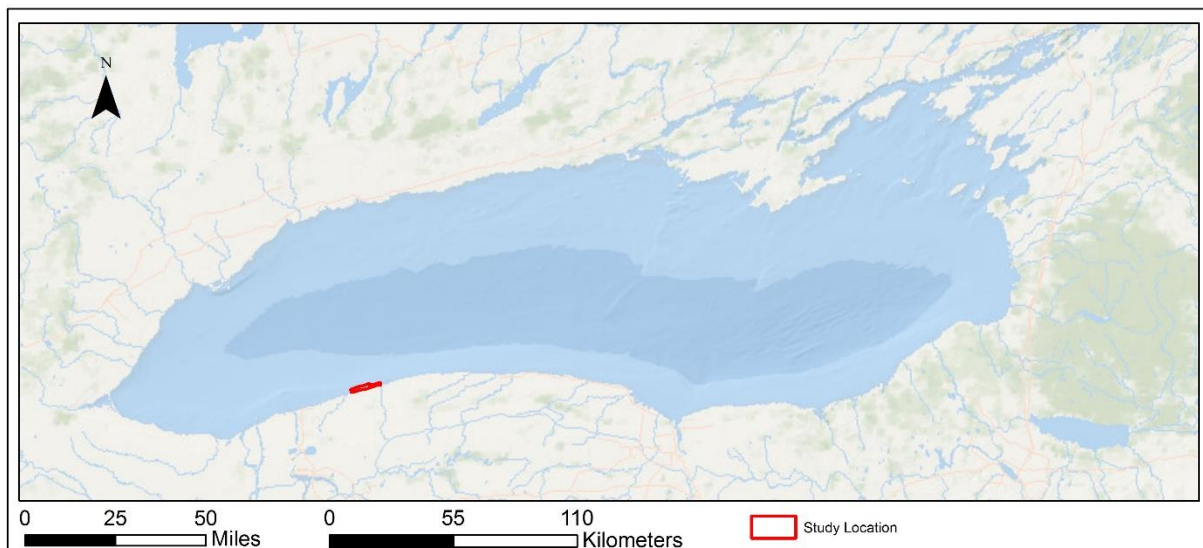


Figure 1: Location of study area for mapping and field observations.

Long-term Annual Time Series

For the long-term time series, the study area was mapped using the Landsat or Sentinel image with the greatest optical depth in the study area for each year from 1975-2019. For several years, the lake bottom was obscured by clouds or turbid water in every image collected during the growing season, resulting in a total of 36 images for the 45-year-long time series. Table 1 summarizes the sources of the annual time series imagery and the major characteristics of the sensors.

Table 1: Sources and satellite characteristics of annual SAV extent maps

SENSOR	PIXEL SIZE (M)	BANDS USED FOR MAPPING	RADIOMETRIC RESOLUTION	YEARS MAPPED
Landsat MSS	60	Green	6 bit	1975-83
Landsat TM	30	Green, blue	8 bit	1984-1999, 2003-2008
Landsat ETM+	30	Green, blue	8 bit	2000-2002
Landsat OLI	30	Green, blue, coastal aerosol	12 bit	2013-2017, 2019
Sentinel-2 MSI	10	Green, blue	12 bit	2018

All imagery except Landsat MSS was atmospherically corrected using the ACOLITE processor (Vanhellemont 2019), which is specifically intended for coastal and inland water applications and uses a dark spectrum fitting approach. Meanwhile, Landsat MSS imagery was converted to top-of-atmosphere radiance, and the effect of the water column was removed by subtracting the average radiance of deep water. Glint was removed based on near-infrared correction (Hedley et al. 2005). Landsat MSS imagery was classified based on the deglinted, deep-water-subtracted green band alone, while for TM, ETM+, and Sentinel-2 MSI imagery, the green and blue bands were used to generate a water-depth-invariant index, the SAV Mapping Algorithm or SAVMA, described in Shuchman et al. (2013). For Landsat OLI, the green, blue, and ultra blue or “coastal aerosol” (435-451 nm) bands were used to generate three depth-invariant indices using the three bands pairs, all of which were inputs for the classification. Sentinel-2 MSI has a similar coastal aerosol band, but it is collected at a coarser resolution (60 m pixels) and so was not used as an input for classification. The 10-m MSI imagery was also resampled to 30 m for the long-term time series so that it would be comparable to the Landsat classifications within one time series.

Figure 2 below summarizes the amounts of lake bottom in the study area classified as SAV or as bare substrate in the images selected for the annual time series. This long-term time series of classified imagery indicates that the percent cover of SAV, which field observations have shown is primarily *Cladophora*, has remained fairly stable at the study site (roughly 2/3 cover) from the mid-1970s to the present, but the surface area of substrate that can be mapped has approximately doubled due to increasing water clarity. This contrasts with the pattern-observed along the Ajax, Ontario shoreline, another time series site on the north side of Lake Ontario (Figure 3), where mappable area has also doubled but where the percentage of lake bottom classified as *Cladophora* has also increased substantially over time. This difference may relate to local drivers such as nutrient sources (Auer 2014).

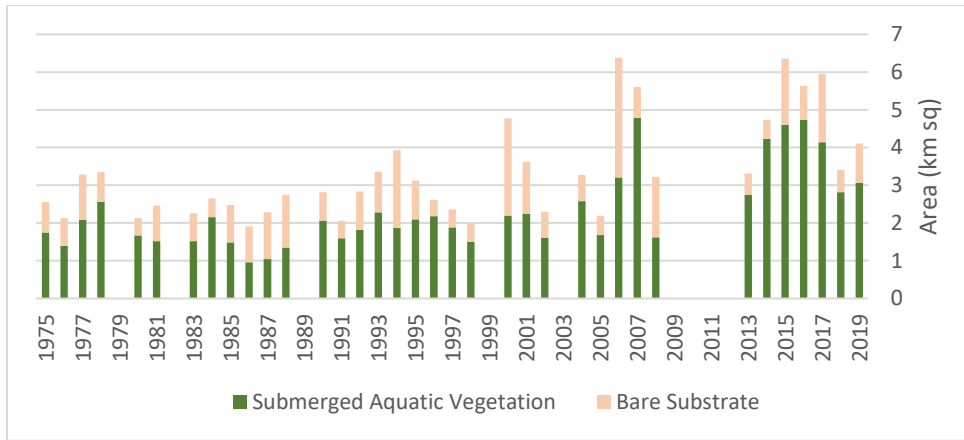


Figure 2: Surface areas of lake bottom in the study area that could be mapped as SAV or as bare substrate in each year's clearest image.

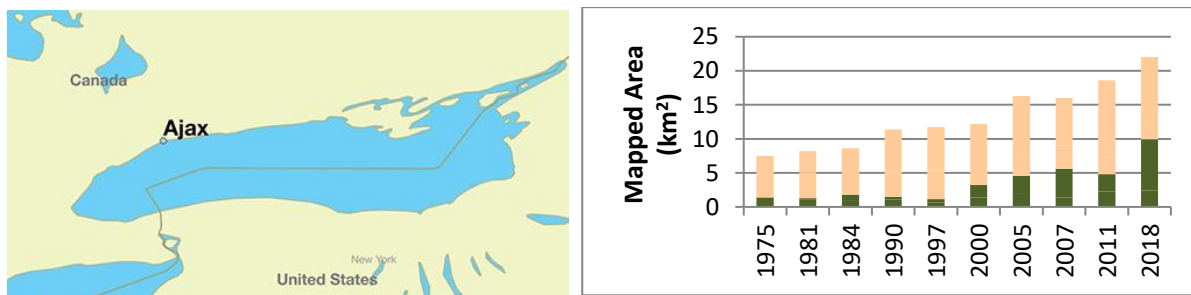


Figure 3: Location and results of time series classification for Ajax study site.

The classification approach used here can also be used to monitor change in water clarity, based on the maximum water depth at which the reflectance from the lake bottom is strong enough for the type of lake bottom to be reliably classified in imagery. This maximum depth, termed the bottom detection depth limit (BDDL) in previous work (Brooks et al. 2015), was calculated for each image in the time series by comparing the lakeward limit of the classification to the USACE NCMP topobathy lidar of the area collected in 2007. The water depth of that elevation at that time was then determined using lake level data from the Great Lakes Water Level Dashboard (Gronewold et al. 2013) to account for the effect of changes in lake level over time. The results are shown in Figure 4.

There was substantial variation in the BDDL from year to year, perhaps due to tributary effects, but the average water clarity clearly increased from approx. 3.5 m in the 1970s to 6 m today. For reference, the approximate time when zebra mussels, which are understood to have had a significant effect on water clarity in the Great Lakes, were introduced to Lake Ontario is also marked on Figure 4. It appears as though the increasing water clarity at the study site may have leveled off in recent years.

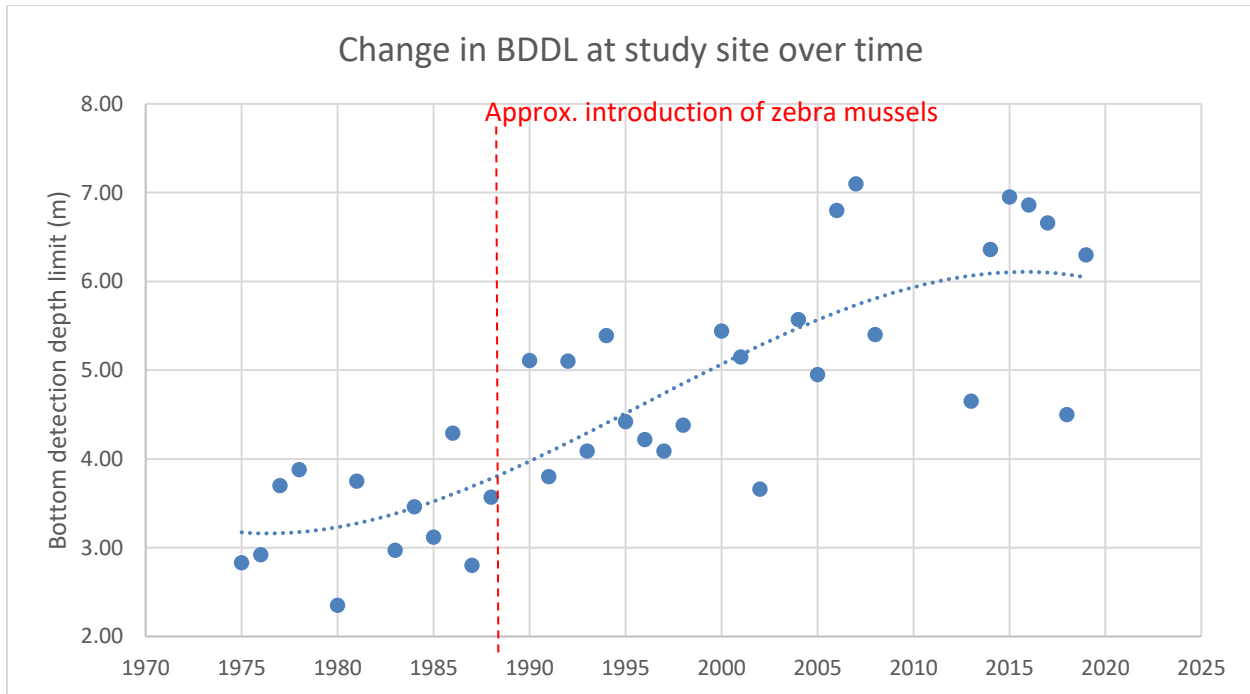


Figure 4: Annual bottom detection depth limit at study site, with trend line.

The Ajax study site on the north side of Lake Ontario exhibits a similar pattern of change in BDDL, increasing from approx. 3.5 m in the 1970s to greater than 8 m today. The pattern of change observed at the study site can also be compared to the Secchi disk measurements collected by the EPA during the same period on research cruises. There are no GLNPO stations very close to the study area that would be similarly influenced by the Niagara River plume, but we can examine two open lake stations in the Niagara Basin, ON25 and ON12 (Figure 5). The GLNPO open lake Secchi measurements show similar interannual variation with a less distinct pattern of increase over time, which is hampered by the limited availability of pre-dreissenid measurements available in the EPA's Great Lakes Environmental Database (GLENDa).

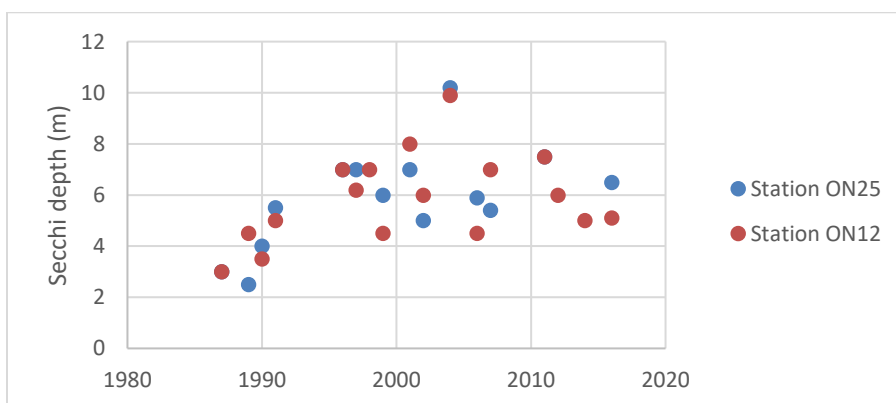


Figure 5: Secchi disk measurements collected during summer GLNPO research cruises at standard GLNPO stations ON25 and ON12.

Seasonal Time Series for 2018 and 2019

For the 2018 and 2019 *Cladophora* growing seasons (April-November), all OLI and MSI images of the study area were downloaded, processed and reviewed. Table 2 summarizes the reasons why much of the collected imagery was not suitable for classification and analysis. Images were considered turbid if known lake bottom features that should be visible in reasonably clear water, such as the shallower shoal that extends into the lake in the center of the study area, were not visible in that image. This left seven high-quality “looks” at the lake bottom in the study area in 2018, and five looks in 2019.

Table 2: Suitability of 2018 and 2019 Landsat OLI and Sentinel-2 MSI for lake bottom mapping.

Year	Sensor	Total images collected April-November	Cloudy	Turbid	Sensor problems	Usable
2018	Landsat OLI	16	12	4	0	0
	Sentinel-2 MSI	97	70	17	3	7
2019	Landsat OLI	16	8	7	0	1
	Sentinel-2 MSI	58	45	9	0	4

Classified Map Validation and Discussion

First, each of the usable images in 2018 and 2019 was processed and classified using the same approach as for the long-term time series. This allowed us to evaluate whether seasonal patterns were present in percent SAV cover (Figure 6a) or water clarity (Figure 6b).

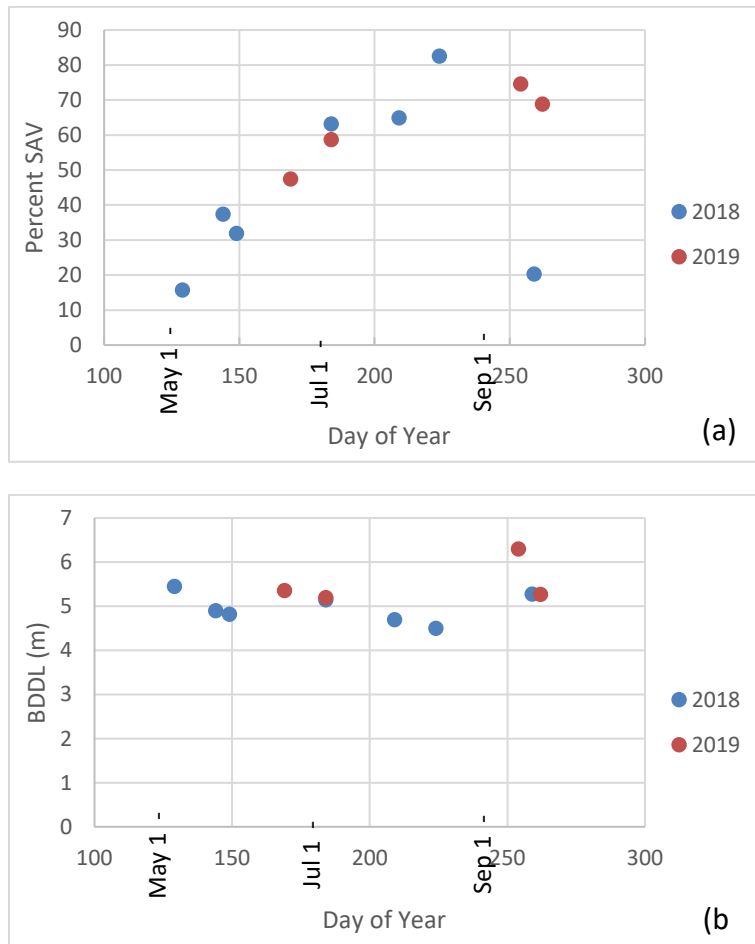


Figure 6: Estimated percent cover of SAV (a) and bottom detection depth limit (b), reflecting water clarity, in the images classified in 2018 and 2019.

The cloud- and turbidity-free Landsat-8 and Sentinel-2 imagery collected during the 2018 and 2019 growing seasons exhibited a distinct seasonal curve in the percentage of the lake bottom classified as SAV, with lower percent cover in the spring and fall and higher cover in the summer. At the same time, the water clarity across the season was fairly stable. In part, though, this is because a number of images showing a very turbid nearshore zone were discarded.

Another way to look at the seasonal pattern of SAV cover is to look at the pixels that were assigned a classification for every usable image and calculate the percentage of images in which they were classified as SAV. This results in a type of heat map that shows where SAV cover was persistently present and where it was more variable. As shown in Figure 7, there was a pattern across both 2018 and 2019 of higher SAV cover (more green) further from shore, with a band of lower SAV cover (redder) along the shoreline. The heat map for 2019 likely looks more uniformly green than 2018 because the 2018 dataset includes 3 images collected in May, before dense *Cladophora* has developed, while the 2019 images are concentrated later in the growing season. The 2018 map might, therefore, more strongly reflect the difference between deeper substrate, where a thin carpet of *Cladophora* remains in place over the

winter, and shallower substrate where much of the senescent *Cladophora* may be removed by ice scour and wave action. At the same time, *Cladophora* generally prefers habitat with a minimum water depth of ~2 m throughout the year due to the harsh conditions of shallower water in the swash and surf zones.

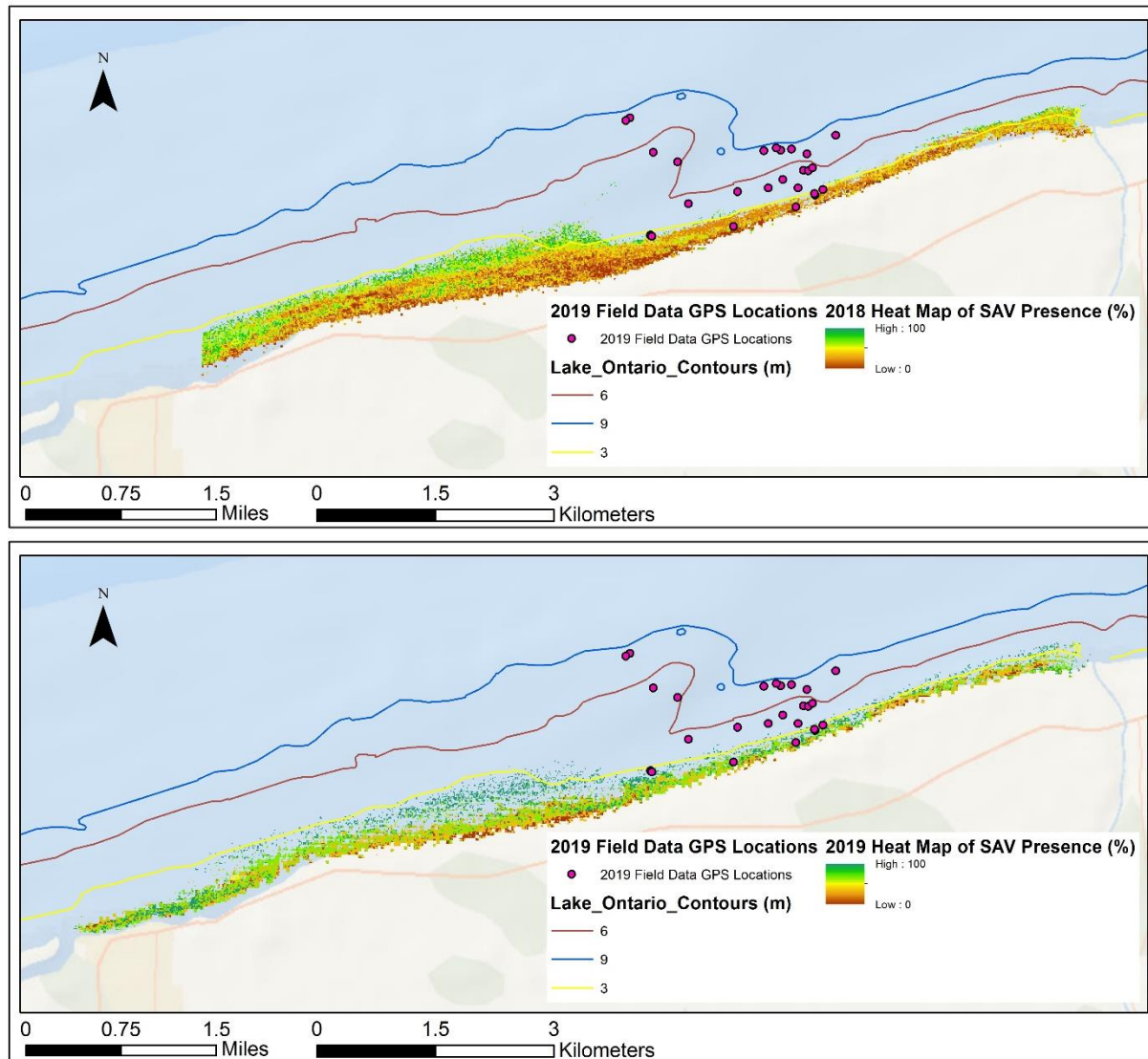


Figure 7: Heat maps of SAV persistence at the study site in 2018 (top) and 2019 (bottom).

The field observations collected in 2019 can also be used to directly evaluate the accuracy of the classified maps generated from satellite images collected near the dates of field observations. The usable satellite imagery includes two close matchups with field dates (18 June field visit vs. 18 June Sentinel-2 image and 31 August field visit vs. 30 August Sentinel-2 image) and a third matchup that is less close but still separated by less than one week (8 July field visit vs. 3 July Sentinel-2 image). Each of these three field dates included estimates of percent cover at 3 m and at 6 m with associated GPS coordinates, for a total of 6 possible validation points. Table 3 summarizes how the field observations

correspond to the classified maps from the corresponding image dates. Both values for 18 June were correct, and the 3 m value for 3-8 July was correct while the lake bottom at the 6 m GPS point was not visible in the image. For 30-31 August, the field and satellite information matched for the 6 m point but not for the 3 m point, which was classified as SAV on 30 August even though the percent cover was estimated at 3% in the field the next day. This difference may have occurred because the field-estimated percent cover represents only *Cladophora*, and the field notes for 31 August state that there was heavy *Spirogyra* growth at both the 3 m and 6 m points. The classified map for 30 August may, therefore, accurately represent that area as heavily vegetated, the vegetation just isn't *Cladophora*, which the satellite algorithm is not designed to distinguish.

Table 3: Comparison of field-estimated percent cover and satellite-based classification at those coordinates for near-coincident dates.

	FIELD POINT AT ~3 M		FIELD POINT AT ~6 M	
	Field % cover	Satellite class	Field % cover	Satellite class
MID-JUNE	18	Uncolonized substrate	50	SAV
EARLY JULY	52	SAV	33	Not visible
END OF AUGUST	3	SAV	76	SAV

As detailed in this report, while field data were collected at 3, 6 and 9 m depths at the study site, nearshore water clarity was typically lower than offshore water clarity due to a strong tributary influence from the Niagara River 35 km to the west. The deepest water in which the type of lake bottom could be classified (bottom detection depth limit, or BDDL) ranged between 4 and 6 m in all of the analyzed 2018 and 2019 satellite images except one (which had a BDDL of 6.3 m). For this reason, for subsequent analyses, satellite-derived products were compared only to the average of the 3 m and 6 m field data, and the satellite products were clipped to the immediate area where the field data were collected and an elevation range from 69 to 72 m asl (approx. 3 to 6 m, Figure 8).

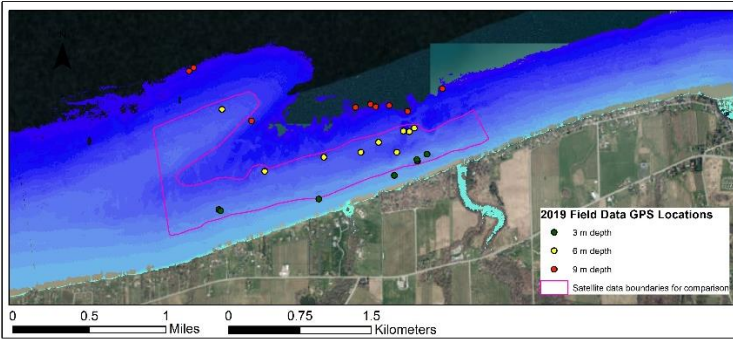


Figure 8: GPS locations of the field data collected in 2019 in water depths of approx. 3, 6 and 9 m, with the polygon boundaries to which the 2019 satellite products were clipped for a more direct comparison of satellite and field values. Background is the 2007 topobathy lidar dataset.

In addition to 1) the (deep-water-subtracted) reflectance in the green band and 2) the SAVMA depth-invariant indices calculated for the classification, 3) the Normalized Coastal Vegetation Index and Normalized Green Vegetation Index were generated and clipped to the area shown in Figure 8. These band indices have been used by other authors for mapping coastal benthic habitats (e.g., Borfecchia et al. 2019), so it was of interest to see whether they produced an interesting signal for *Cladophora* in this context. They were calculated similarly to the more commonly used NDVI as follows:

$$\text{Normalized Coastal Vegetation Index (NCVI)} = (b1 - b2) / (b1 + b2)$$

$$\text{Normalized Green Vegetation Index (NGVI)} = (b3 - b2) / (b3 + b2)$$

where b1, b2 and b3 are the coastal aerosol, blue and green bands, respectively.

Green Reflectance

Because growing green vegetation is less reflective at green wavelengths than uncolonized lake substrate, we would expect that green reflectance would be lower during peak SAV growth than early or late in the growing season. That is the general pattern we see in the seasonal time series for green reflectance in the clipped study area (Figure 9), especially in 2018, when a few more images are available to help distinguish the pattern. The same approximate range of values also occurs in both years, which helps confirm that the ACOLITE atmospheric correction and deglinting preprocessing is producing reliable results. Both years also show an increase mid-season followed by a decrease to a new local minimum, which could reflect a sloughing event, but more imagery would be needed to provide a better understanding of day-to-day variation to confirm that. Also, the field observations for 2019 did not capture a significant sloughing event in 2019.

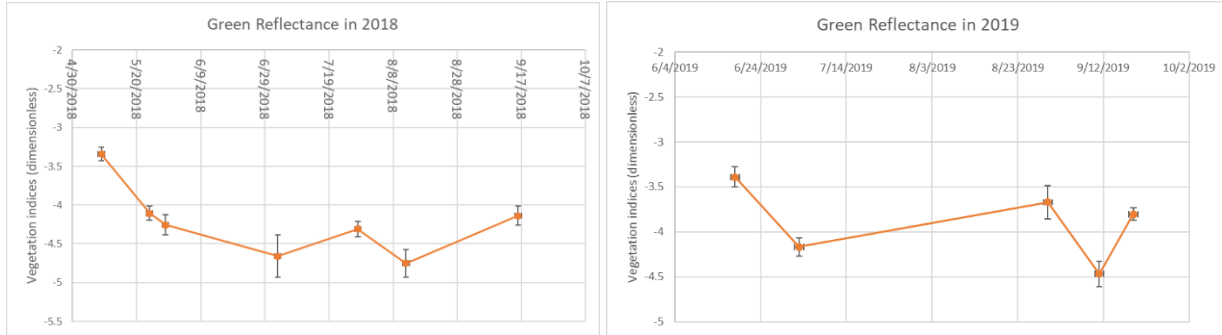


Figure 9: Green reflectance within area outlined in Figure 8 in Landsat/Sentinel imagery from 2018 and 2019. Error bars represent standard deviation.

When green reflectance is compared to measured percent cover and dry biomass for the three dates on which field data and usable satellite imagery were coincident or near-coincident, we again see approximately the pattern we would expect, where a higher percent cover or biomass of SAV is associated with a lower reflectance value (Figure 10). Additional field/satellite matchups would be needed to have confidence in this pattern.

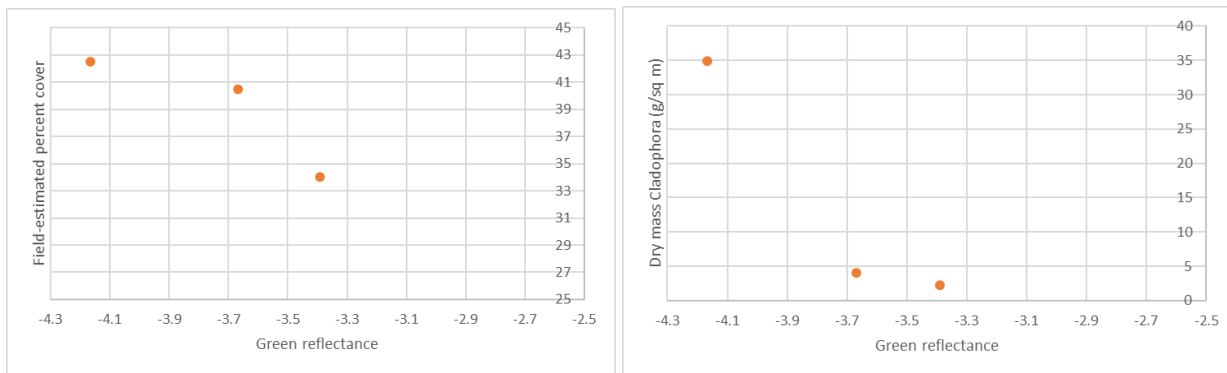


Figure 10: Satellite-based green reflectance from the lake bottom vs. field-estimated percent cover (left) and dry mass (right) for near-coincident dates in 2019 (average of point measurements collected at approx. 3 and 6 m).

Vegetation Indices

The expectation for the NCVI and NGVI vegetation indices is that they would be higher when the percent cover of SAV is higher, but looking at Figure 11, the range of variation of these indices was fairly small relative to their standard deviations. On the right side of Figure 11, the field observations of percent cover are plotted on top of the vegetation indices, and there is no clear pattern of correspondence for NGVI. NCVI does increase from late June to early July along with the percent cover, then drops significantly at the end of August at the same time that percent cover does, but more investigation into the utility of this index is needed.

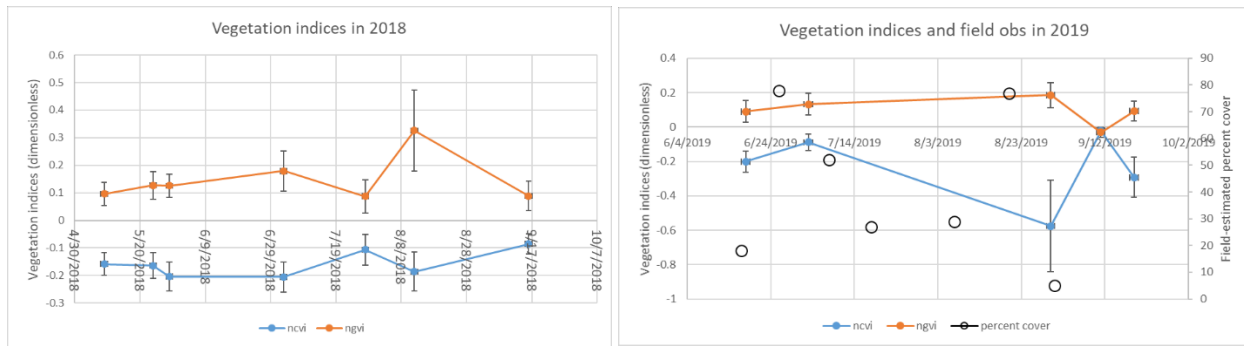


Figure 11: Mean and standard deviation of NCVI (blue) and NGVI (orange) values within area outlined in Figure 8 calculated from Landsat/Sentinel imagery from 2018 (left) and 2019 (right). Field-estimated percent cover is also overlaid on the 2019 plot.

SAVMA Depth-Invariant Indices

The three calculated SAVMA indices all tended to be higher during the peak of the growing season and showed smaller standard deviations among pixels than the vegetation indices (Figure 12). The index using bands 1 and 3 showed the largest range of values in both years, which is intuitive as of the three spectral bands, bands 1 and 3 are the two that are farthest apart on the EM spectrum. Notably, the ranges of values for the two years are quite different, with di_{13} ranging from approx. (-2) to 35.5 in 2018 vs. (-4) to 4 in 2019. The reason for this large difference between years is not clear without field data for 2018. When the di indices are compared to measured percent cover and dry biomass for the three dates on which field data and usable satellite imagery were coincident or near-coincident (Figure 13), the values trend in the expected direction, but again, more data would be valuable to confirm or dispel the apparent pattern.

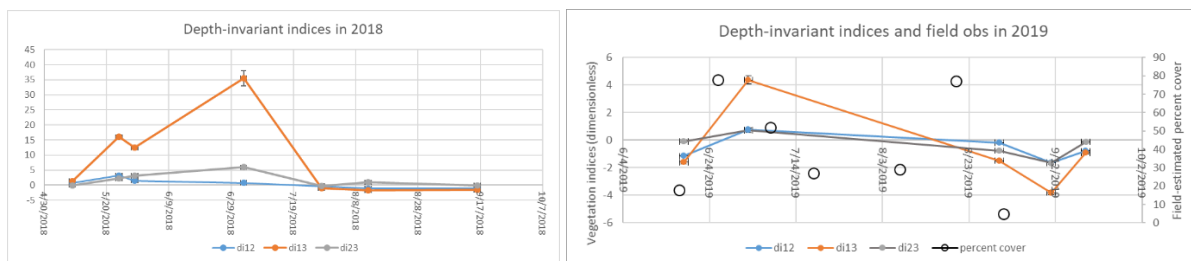


Figure 12: Mean and standard deviation of di_{12} (blue), di_{13} (orange) and di_{23} (gray) values within area outlined in Figure 8, calculated from Landsat/Sentinel imagery from 2018 (left) and 2019 (right). Field-estimated percent cover is also overlaid on the 2019 plot.

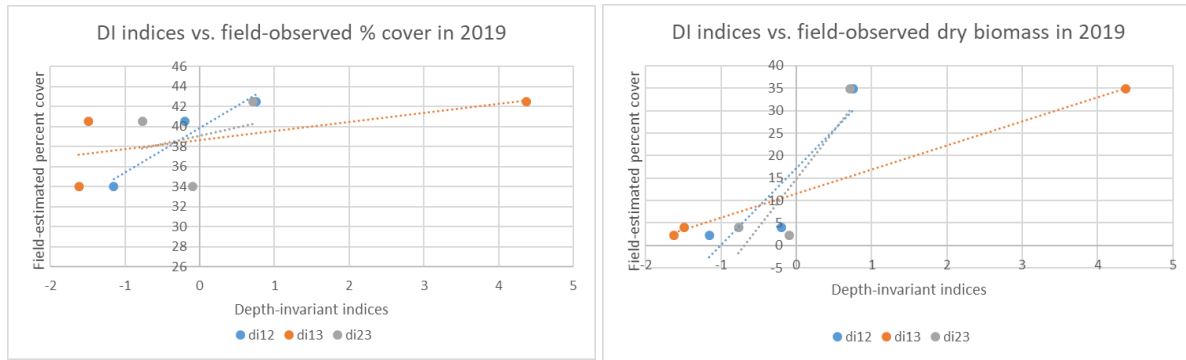


Figure 13: Satellite-based SAVMA depth-invariant indices vs. field-estimated percent cover (left) and dry mass (right) for near-coincident dates in 2019 (average of point measurements collected at approx. 3 and 6 m).

Discussion

The type of mapping using SAVMA depth-invariant indices presented here has previously been validated and published (Shuchman et al. 2013, Brooks et al. 2015), but coincident field data were not available for that work. Here, the combination of multispectral satellite imagery, now freely available for the Great Lakes at a higher frequency thanks to the combination of Landsat-8 OLI and Sentinel-2 MSI, and several field visits to the same site within a single year allowed us to begin exploring the limits of this type of satellite data for measuring water clarity, SAV distribution and SAV biomass in the coastal Great Lakes. While near-coincident satellite matchups were only available for three of the nine dates of field observations in 2019, there was generally good agreement between the patterns observed in the field and via satellite with respect to water clarity and *Cladophora* growth patterns. The field data were also useful for contributing to the validation of the classified maps generated from the di indices. At the same time, this work highlighted some of the limitations of the satellite approach, such as the inability to distinguish between *Cladophora* and *Spirogyra* growth within *Cladophora* beds.

As a next step, we plan to develop these results into a manuscript for submission to a peer-reviewed journal, with additional analysis related to the interactions between water clarity, *Cladophora* growth requirements and limits, and mapped lake bottom type.

References

Auer, M. T. (2014). Field Studies of Phosphorus and *Cladophora* in Lake Ontario Along the Ajax, Ontario Waterfront. In *Report to the Town of Ajax, Ontario*.

Borfecchia, F., Consalvi, N., Micheli, C., Carli, F. M., Cognetti De Martiis, S., Gnisci, V., ... & Marcelli, M. (2019). Landsat 8 OLI satellite data for mapping of the *Posidonia oceanica* and benthic habitats of coastal ecosystems. *International Journal of Remote Sensing*, 40(4), 1548-1575.

Brooks, C., Grimm, A., Shuchman, R., Sayers, M., & Jessee, N. (2015). A satellite-based multi-temporal assessment of the extent of nuisance *Cladophora* and related submerged aquatic vegetation for the Laurentian Great Lakes. *Remote Sensing of Environment*, 157, 58-71.

Gronewold, A. D., Clites, A. H., Smith, J. P., & Hunter, T. S. (2013). A dynamic graphical interface for visualizing projected, measured, and reconstructed surface water elevations on the earth's largest lakes. *Environmental Modelling & Software*, 49, 34-39.

Hedley, J. D., Harborne, A. R., & Mumby, P. J. (2005). Simple and robust removal of sun glint for mapping shallow-water benthos. *International Journal of Remote Sensing*, 26(10), 2107-2112.

Shuchman, R. A., Sayers, M. J., & Brooks, C. N. (2013). Mapping and monitoring the extent of submerged aquatic vegetation in the Laurentian Great Lakes with multi-scale satellite remote sensing. *Journal of Great Lakes Research*, 39, 78-89.

Vanhellemont, Q. (2019). Adaptation of the dark spectrum fitting atmospheric correction for aquatic applications of the Landsat and Sentinel-2 archives. *Remote Sensing of Environment* 225, 175–192. (<https://doi.org/10.1016/j.rse.2019.03.010>)